A boundary condition to control acoustic reflexion for turbomachinery aeroelasticity

Nicolas Cortes, Alain Dugeai

A BOUNDARY CONDITION TO CONTROL ACOUSTIC REFLEXION FOR TURBOMACHINERY AEROELASTICITY

Nicolas Cortes and Alain Dugeai
DAAA, ONERA, Université Paris Saclay, Châtillon, France
email: cortes.nicolas@onera.fr

The fan of an aeronautic engine may experience aeroelastic instabilities called flutter. This phenomenon is the source of large vibrations which can lead to fatigue and even fracture. Moreover, this instability can be triggered by acoustics. By vibrating, the fan emits acoustic waves that propagate within the air intake under specific conditions. These waves are reflected at the air intake lips and they return to the fan. By modifying the instantaneous pressure acting on the fan, the waves change the aerodynamic damping which may lead to an aeroelastic instability.

In the present study, this phenomenon has been studied numerically on a simplified configuration. It consists of a 6 blades fan placed in an annular duct. The link between structural modes and acoustic modes has been highlighted. Indeed, each structural mode can lead to several acoustic modes, but all acoustic waves can not propagate in the air intake. In order to propagate, their frequency must be higher than their cut-on frequency, which limits the number of harmonics. The evolution of the aerodynamic damping with the air intake length has then been investigated. It has been observed that the aerodynamic damping is depending on the phase of the returning acoustic wave.

However, this phenomenon is also related to the acoustic properties of the inlet boundary condition. Therefore, a specific boundary condition capable of controlling the reflection of an acoustic wave at inlet has been developed. This boundary condition is based on the 2D method of characteristics formulated by Giles. Such a condition allows reducing the size of the fluid domain in CFD simulations by modelling the reflection instead of calculating it numerically by considering a large fluid domain surrounding the engine inlet. The implementation of the condition is detailed, and applications showing its effectiveness are presented and discussed.

Keywords: aeroelasticity, boundary condition, turbomachinery, duct acoustic

1. Introduction

The fan of a turbojet may experience aeroelastic instabilities leading to fatigue or even fracture. It is then crucial to be able to predict numerically the conditions inducing such instabilities. This phenomenon is named flutter. It is caused by a coupling between the fluid and the structure. When the structure is moving, the flow around the blade is modified, as a consequence the pressure on the blade is also changed. It results in an exchange of energy between the fluid and the structure. If energy is provided by the fluid to the blade structure, the movement of the blade is exponentially amplified. This amplification can be detected by a negative aerodynamic damping evaluated in forced motion. Aircraft engine manufacturers enhance the bypass ratio of their turbojet by increasing the size of the fan and reducing the length of the air intake. It increases the risk of flutter as the blades are more flexible. Moreover, this tendency encourages the reflexion of acoustic waves at the air intake lips which may provoke an anticipated entry into the flutter domain. This phenomenon of flutter triggered by acoustic is named the flutter

bite. When the fan is oscillating, acoustic waves are emitted. Under some conditions, these waves propagate upwind and eventually reach the air intake lips. There, the waves are reflected and return toward the fan. By modifying the instantaneous pressure around the blade, the acoustic waves can increase or decrease the aerodynamic damping. In the industry, the fluid domain used in numerical simulations is limited to the engine inside the nacelle which requires the use of an inlet boundary condition. However, the boundary conditions available in elsA, Airbus-SAFRAN-ONERA's CFD code [1], are not able to correctly describe the acoustic reflexion at the air intake. Therefore, the stability limit cannot be well predicted. An alternative solution is to simulate a larger domain surrounding the turbojet in order to calculate the reflexion through the CFD [2]. But this method comes with tremendous simulation costs.

The objective is to develop a boundary condition capable of controlling the reflexion of acoustic waves at the air intake. This boundary condition is intended to model the reflexion in order to correct the damping calculation without increasing the domain of simulation.

This paper begins with a study of an academic configuration of turbofan. In this second section, the effect of a classical injection boundary condition on the aerodynamic damping is observed. Then, the development of the new boundary condition is presented. Finally, the new boundary condition is confronted to the previous injection condition in order to highlight the improvement.

2. Study of an academic configuration of turbofan

The configuration under study is composed of two coaxial cylinders. One represents the shroud while the other represents the carter. Six blades are placed in between as a fan. However, there is no OGV as the study is limited to the upwind part. The blades have no thickness. The physical parameters are inspired from an industrial fan demonstrator. The shroud radius R_m is 45cm and the carter radius R_c is 90cm. The downstream length is supposed infinite but the upstream length L is a parameter that has been varied from 8.25m to 10m. The operating point of the fan chosen for this study is the point of mass flow $\dot{m} = 200kg/s$ and of pressure ratio $RPI = 1.13$. This point corresponds to an inlet at the standard atmosphere conditions, a rotation speed $\Omega_R = 320rad/s$ and an outlet pressure $P_{out} = 107000Pa$. Within these conditions, the fan is forced to vibrate at a frequency $f_{blade} = 100Hz$.

The vibration of the blades produces acoustic waves which take the form of duct modes. Duct modes (m, μ) are described by an azimuthal wave number m and a radial wave number μ. It means that in a duct section, areas of higher and lower pressure are separated by nodal diameter and nodal circle. Each mode has a cut-on frequency. If the frequency of the wave is higher than its cut-on frequency, the wave propagates. The structural modes chosen to produce the acoustic wave are first flexion blade mode with a proper value of inter-blade phase angle to select particular azimuthal wave numbers (Fig. 2). As a consequence, only acoustic modes with $\mu = 0$ have been studied. As no stiffness is associated to the structural modes, the exact value of damping can not be calculated and therefore the values of damping are not indicated on the following figures.

2.1 Numerical setup

First, let us briefly recall the main features of the elsA software. The elsA multi-application CFD simulation platform deals with internal and external aerodynamics from the low subsonic to the high supersonic flow regime and relies on the solving of the compressible 3-D Navier-Stokes equations. elsA allows the simulation of the flow around moving deformable bodies in absolute or relative frames. Complex geometrical configurations may be handled using high flexibility techniques involving multi-block structured body-fitted meshes. The system of equations is solved by a cell centered finite-volume method.

Space discretization schemes include classical second order centered or upwind schemes and higher order schemes. The mostly used integration of the semi-discrete equations relies on a backward Euler technique with implicit schemes solved by robust LU relaxation methods. [1]

As the dynamic of the structure is imposed, only the fluid has been meshed. The mesh is structured and multi-blocks. It is regular in the upstream part with 20 points per meter. However, the mesh axial discretization is progressive in the downstream part in order to numerically damp the acoustic wave and avoid as much as possible the reflexion at the outlet. The total number of points is around 500 000. A plot of the mesh is presented in Fig. 1.

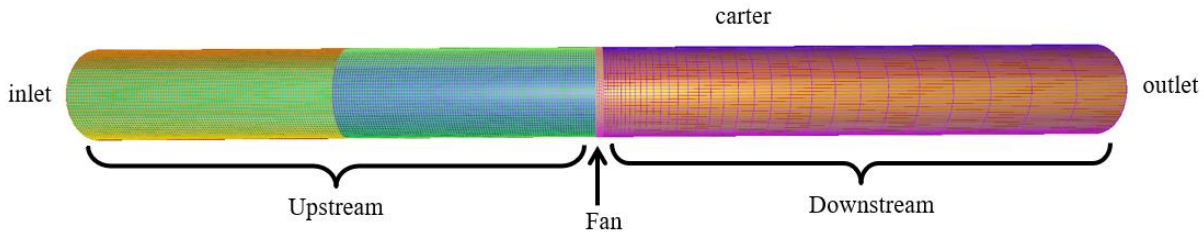

Figure 1: Mesh used for the aeroelastic simulations.

The blades do not appear in the mesh because they do not have any thickness. To take them into account, wall slip conditions have been placed at the interface of two blocks. Then, to make the blades oscillate, the blade boundaries are moved according to the structural mode represented in Fig. 2, the volumic mesh is then deformed accordingly using a structural analogy. At the inlet, a boundary condition of "injection" has been used. The total pressure, the total enthalpy and the direction of the velocity are given by the user. The condition applies the characteristic relations to find the static pressure, the velocity and the density. At the subsonic outlet, according to characteristic relations, the BC only requires the static pressure value. The other variables are calculated by the characteristic relations. Wall slip conditions are used at the shroud and the carter.

The CFD solver elsA used here allows to do aeroelastic simulations in forced motion. The Euler equations are solved. It means there is no viscosity, no boundary layer and no turbulence. The amplitude of the forced motion is small (1mm) in order to avoid non-linear effects. The Roe spatial scheme is used by the CFD solver. For time integration, the Dual Time Stepping (DTS) method is used to advance in time. The temporal discretisation is 128 time steps per vibration period and the simulations run for a total time of 30 periods.

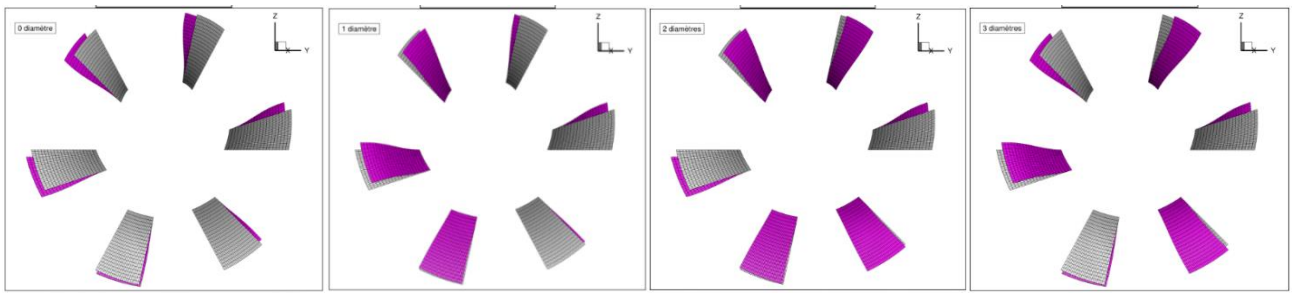

(a) Mode 0 (b) Mode 1 (c) Mode 2 (d) Mode 3

Figure 2: Real part of the deformed shape (violet) compared to the reference shape (grey) for modes of a 6 blades fan.

2.2 Results with an injection boundary condition

First, it's possible to visualise the unsteady static pressure. An extraction of the conservative variables has been performed on a 0.7 m radius cylindric surface and at the inlet plan. The pressure perturbations from the mean field is plotted in Fig. 3 for two modes. In Fig. 3a, the pressure perturbation for the (0,0) acoustic mode generated by the 0-diameter structural mode is exhibited. The case of the (2.0) pressure mode triggered by mode 2, is shown on Fig. 3b. In the two cases, the waves are propagating downstream and upstream. The acoustic mode (0,0) is a plane wave but all the other acoustic modes are propagating with an helicoidal pattern. Furthermore, in the upstream part, interference figures can be observed. It results in stationary waves in the axial direction but still rotating around the axial axis.

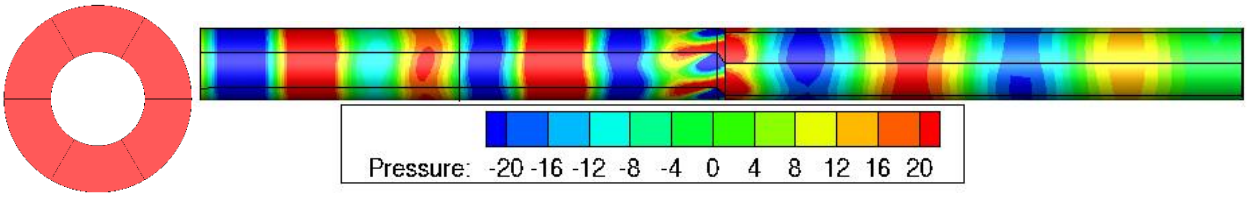

(a) Mode 0

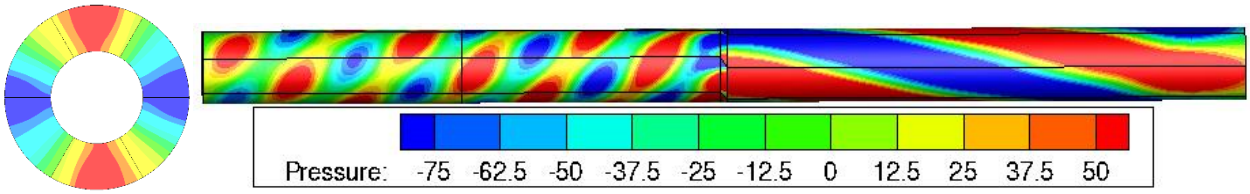

(b) Mode 2

Figure 3: Pressure perturbation field induced by (a) the mode 0 and (b) the mode 2 of structure. At the left, the extraction at the inlet plan and at the right, the extraction on the 0.7m radius cylindric surface.

The principal interest of the CFD aeroelastic simulation is to give access to the aerodynamic damping of the structural modes in order to evaluate the risk of flutter. The evolution of the damping is plotted for several structural modes in the Fig. 4 left. The aerodynamic damping begins to converge toward a value without reflexion but when the reflected acoustic wave reaches the fan (for example period 7, for mode 0, see Fig. 4 left), the damping is modified. The modification of the damping does not occur at the same moment for all the modes because each acoustic mode has its own wave speed (Fig. 4 left).

Moreover, it can be observed that the damping modification is sometimes positive and sometimes negative. In Fig. 4 right, the final damping has been plotted as a function of the length of the upstream part. The line "ref" is obtained with the injection boundary condition that reflects the acoustic waves while the line "ssref" gives the reference value of damping obtained with a simulation with a degressive mesh at the upstream to avoid the reflection.

First, it can be noted that each structural mode has not the same aerodynamic damping even without reflexion. It is due to the interaction between the blades that are not the same from a mode to another because of the different values of the inter-blade phase angle. This figure highlights oscillations with the upstream duct length of the damping about a mean damping value, corresponding to the no-reflexion case. Depending on the length travelled by the wave, the reflected wave reaches the blades with a different phase that increases or decreases the damping. Vahdati et al. already observed this phenomenon for the reflexion of acoustic waves in [3,4]. The amplitude of the modification of the damping depends on

the mode but it is not negligible. This study shows that the classical injection boundary condition used at inlet may lead to erroneous values of the aerodynamic damping, depending on the length of the inlet duct modelled.

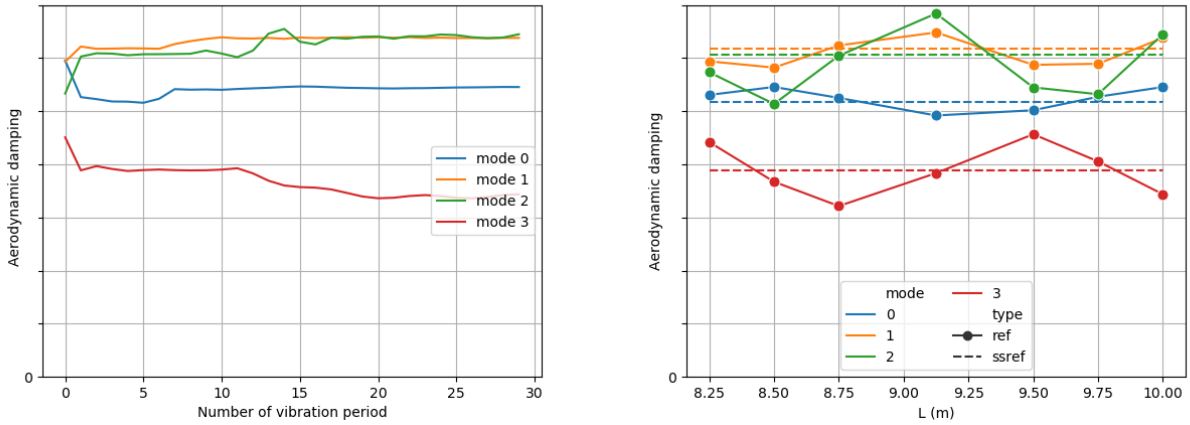

Figure 4: Aerodynamic damping for 4 modes of structure (left) during the simulation with L=10m (right) at the end of the simulations depending on the upwind length L.

3. Non-reflecting boundary condition

To improve the robustness of the prediction of the aerodynamic damping, the development of a non-reflecting boundary condition is considered. This boundary condition is based on the unsteady Giles' theory [5] for a single, known-in-advance frequency.

3.1 The Giles' theory

Giles begins with a linearization of the Euler equations expressed in primitive variables:

$$\frac{\partial \widetilde{U}}{\partial t} + A\frac{\partial \widetilde{U}}{\partial x} + B\frac{\partial \widetilde{U}}{\partial y} = 0 \tag{1}$$

His theory deals with the perturbations, the mean part needs to be processed separately with conventional methods. Then, Giles supposes that the acoustic waves are 2D and take the following form:

$$\widetilde{U} = \tilde{u}e^{i(kx+ly-\omega t)} \tag{2}$$

The Euler perturbation equations becomes:

$$(-\omega I + kA + lB)\tilde{u} = 0 \tag{3}$$

In presence of acoustic waves, the perturbation is not zero. As a consequence, the relation of dispersion must be verified:

$$\det(-\omega I + kA + lB) = 0 \tag{4}$$

The roots of this polynomial function of k are the wave numbers of the characteristics. Due to the 2D waves hypothesis, the wave numbers found by Giles are a bit different from the wave numbers found by Rienstra in [6] who considers the radial dependency of the waves. In the following the wave numbers of Rienstra are used. To find non-reflecting relations, the left vector of the kernel v_n^L of the matrix $-\omega A^{-1} + k_n I + lA^{-1}B$ has to be found. These vectors permit to express the non-reflecting relations with orthogonality relations. The vector of primitive variables $\widetilde{U}$ can be written has a superposition of waves:

$$\widetilde{U} = \left[\sum_{n=1}^{N} a_n u_n^R e^{ik_n x}\right] e^{i(ly-\omega t)} \tag{5}$$

where u_n^R are the right vector of the kernel that verify Eq. (3).

The non-reflecting relations consist of taking $a_n = 0$ for the waves entering the domain. It can be written as:

$$v_n^L \widetilde{U} = a_n (v_n^L u_n^R) e^{ik_n x} e^{i(ly-\omega t)} = 0 \tag{6}$$

for n corresponding to an entering wave.

As the relation is only for waves entering the domain, it is easier to write it in terms of characteristics with $\widetilde{U} = M_\phi \widetilde{\Phi}$ where is a matrix calculate primitive variables from characteristics:

$$\widetilde{\Phi}_{2D,n} = (v_n^L M_\phi)\widetilde{\Phi} = 0 \tag{7}$$

Thus, it is possible to deduce the entering characteristics from the leaving characteristics. For example, for an inlet in subsonic flow, the non-reflecting relation is:

$$\begin{pmatrix} \tilde{\phi}^{vorticity,\theta} \\ \tilde{\phi}^{entropy} \\ \tilde{\phi}^{+} \end{pmatrix} = \begin{pmatrix} G * \tilde{\phi}^{-} \\ 0 \\ G^2 * \tilde{\phi}^{-} \end{pmatrix} \tag{8}$$

where G is a coefficient derived by Giles in his paper [5], which depends on the mean velocities, l and ω.

3.2 Results

As in Section 2.2, the aerodynamic damping is plotted as a function of the upstream length. Figure 5 left shows the results given by the new boundary condition under the hypothesis of plane wave (G=0). The mode 0 and 1 are independent of the upstream length which means that the acoustic waves are not being reflected. For mode 2 and 3, there is still some variation because these modes have a more 2D shape. Then, in Fig. 5 right, the Giles' theory is applied at the inlet. With this new boundary condition, all the modes tested are independent of the upstream length. These acoustic waves are not reflected anymore and the boundary condition behaves as expected.

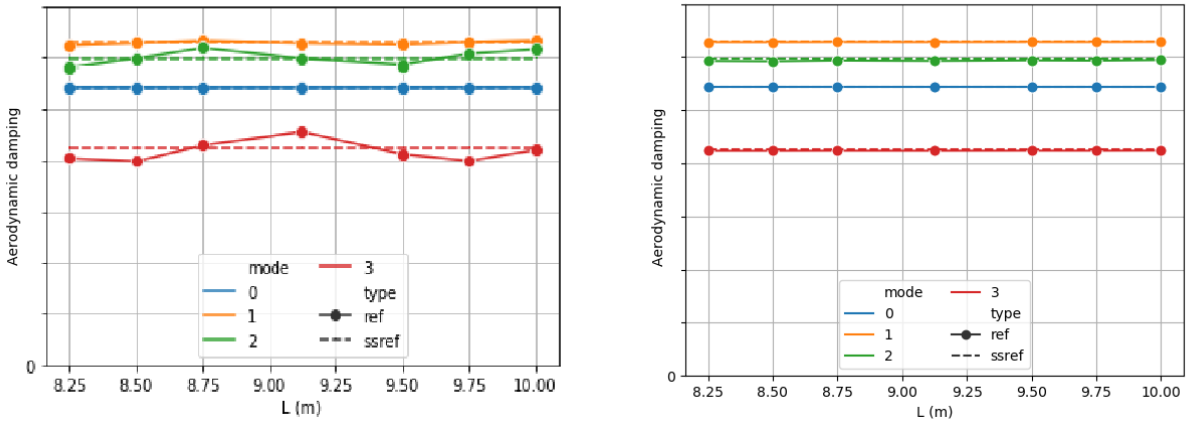

Figure 5: Aerodynamic damping for 4 modes of structure depending on the upwind length L with (left) the plane wave hypothesis and (right) the Giles' theory.

The limitation of this non-reflecting boundary condition is that it is 2D. Waves with a radial wave number are 3D and then the boundary condition is not correctly absorbing such waves. Furthermore, when the

upstream length is very short, the acoustic waves do not have enough space to take the analytical form that is supposed in the theory.

4. Impedance boundary condition

Now that the undesired reflection has been avoided, it is possible to reinject a pressure wave in function of the leaving pressure wave. Such a boundary condition may be useful to model a physical reflexion of pressure waves.

4.1 Method

In [7], Kaess et al. already developed an impedance boundary condition based on the NSCBC method that reflects planar waves by simulating an impedance through a complex reflection factor $R = Ae^{i\beta}$.

For planar waves, the reflection relations for an inlet are thus:

$$\begin{pmatrix} \tilde{\phi}^{vorticity,\theta} \\ \tilde{\phi}^{entropy} \\ \tilde{\phi}^{+} \end{pmatrix} = \begin{pmatrix} 0 \\ 0 \\ R * \tilde{\phi}^{-} \end{pmatrix} \tag{9}$$

In the present paper, a combination of the non-reflective boundary condition of Giles and an impedance boundary condition has been implemented. The relations used are:

$$\begin{pmatrix} \tilde{\phi}^{vorticity,\theta} \\ \tilde{\phi}^{entropy} \\ \tilde{\phi}^{+} \end{pmatrix} = \begin{pmatrix} G * \tilde{\phi}^{-} \\ 0 \\ G^2 * \tilde{\phi}^{-} \end{pmatrix} + \begin{pmatrix} 0 \\ 0 \\ R * \tilde{\phi}^{-} \end{pmatrix} \tag{10}$$

4.2 Results

This boundary condition has been tested on a shorter configuration (L=2m) with a fan composed of 18 blades. The parameter β of the reflecting factor has been varied from 0° to 360° while keeping the same upstream length. Figure 6 can not be directly compared with the previous ones because it is another configuration on another operating point. The oscillation of the damping around the value without reflection for all the modes highlights the fact that the phase of the reflecting wave has been modified.

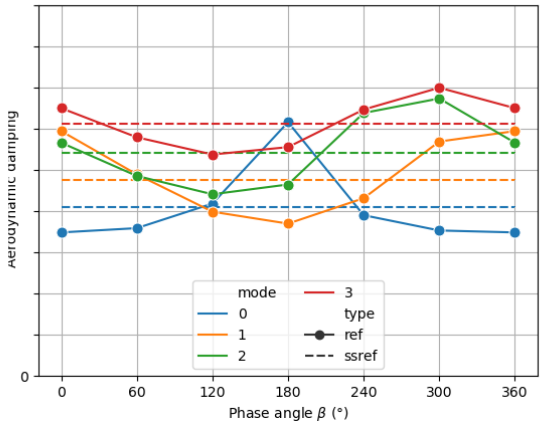

Figure 6: Aerodynamic damping for 4 modes of structure depending the parameter β of the reflecting factor.

To completely validate this boundary condition, the reflection factor should be determined by an acoustic code or by experience and given to the boundary condition in order to compare the damping against reference data like experimental data or CFD simulations with a fluid domain all around the turbofan.

5. Conclusion

The fan of a turbojet may experience aeroelastic instabilities called flutter, leading to fatigue or even fracture. Flutter can be facilitated or hampered by acoustic interactions with the air intake. Simulations on an academic configuration have permitted to observe the evolution of the damping with the upstream length and with the acoustic modes at stakes. It appears that the aerodynamic damping depends on the phase of the acoustic wave returning on the fan. In order to avoid the use of large fluid domains around the turbojet, an impedance boundary condition has been developed. It is based on the Giles' theory to avoid undesirable reflection and it uses a reflection factor to calculate the characteristics of the entering wave from the leaving wave.

This new boundary condition still needs further validations. It has to be tested in industrial geometry and with URANS simulations. Some further improvement can be considered. An expression for the reflexion relations has been written in 2D but needs to be numerically tested. Finally, in the boundary condition developed in this paper, the waves are reflected in the same duct mode but it would be relevant to allow the waves to reflect in other duct modes.

REFERENCES

1 Cambier, L., Heib, S., and Plot, S., The Onera elsA CFD software: input from research and feedback from industry, *Mechanics & Industry* **14** (3) (2013): 159-174.

2 Bontemps, T., Aubert, S., and de Pret, M., Prediction of the acoustic reflection in a realistic aeroengine intake with three numerical methods to analyse fan flutter, *Journal of Turbomachinery*, **143** (10), (2021).

3 Vahdati, M., Simpson, G., and Imregun, M., Mechanisms for wide-chord fan blade flutter, *Journal of Turbomachinery*, **133** (4), (2011).

4 Zhao, F., Smith, N., and Vahdati, M., A simple model for identifying the flutter bite of fan blades, *Journal of Turbomachinery* **139** (7) (2017): 071003.

5 Giles, Michael. *Non-reflecting boundary conditions for the Euler equations*. Cambridge, MA, USA: Computational Fluid Dynamics Laboratory, Department of Aeronautics and Astronautics, Massachusetts Institute of Technology, 1988.

6 Rienstra, S. W., Fundamentals of duct acoustics, *Von Karman Institute Lecture Notes*, (2015).

7 Kaess, R., Huber, A., and Polifke, W., A time-domain impedance boundary condition for compressible turbulent flow, *14th AIAA/CEAS Aeroacoustics Conference (29th AIAA Aeroacoustics Conference)*, page 2921, (2008).